International Journal of Pharmaceutics 397 (2010) 155–163

Contents lists available at ScienceDirect

International Journal of Pharmaceutics

journal homepage: www.elsevier.com/locate/ijpharm

Pharmaceutical Nanotechnology

Wheat germ agglutinin-grafted lipid nanoparticles: Preparation and *in vitro* evaluation of the association with Caco-2 monolayers

Ying Liu [a], Pengfei Wang [a], Chen Sun [a], Nianping Feng [a,*], Wuxiong Zhou [b], Yang Yang [b], Rong Tan [a], Zhiqiang Chen [a], Shan Wu [a], Jihui Zhao [a]

[a] *Department of Pharmaceutics, School of Pharmacy, Shanghai University of Traditional Chinese Medicine, Shanghai 210203, PR China*
[b] *Experiment Center for Science and Technology, Shanghai University of Traditional Chinese Medicine, Shanghai 201203, PR China*

ARTICLE INFO

Article history:
Received 15 March 2010
Received in revised form 12 June 2010
Accepted 18 June 2010
Available online 25 June 2010

Keywords:
Wheat germ agglutinin
Lipid nanoparticles
Caco-2 monolayers
Oral drug delivery

ABSTRACT

A bioadhesive drug delivery system, wheat germ agglutinin (WGA)-grafted lipid nanoparticles, was developed for the oral delivery of bufalin (a hydrophobic active component extracted from the traditional Chinese medicine *Chan'su*). The lipid nanoparticles associated with poly(vinyl alcohol) (PVA) were prepared by high-pressure homogenization. WGA was coupled to lipid nanoparticles by activating the hydroxyl group using glutaraldehyde, and then conjugating the nanoparticles with WGA. WGA-grafted lipid nanoparticles with a mean particle size of 164 nm and zeta potential of −10.6 mV were obtained with bufalin encapsulation of 68.2%. The amount of bound WGA was ~28.9% of the amount of WGA initially added. The association study between fluorescent 6-coumarin-loaded WGA-grafted lipid nanoparticles and Caco-2 monolayers showed that WGA enhanced the cellular uptake of nanoparticles compared with WGA-free lipid nanoparticles. These results suggest that WGA-grafted lipid nanoparticles could be a promising carrier to enhance cellular uptake. They could also improve drug bioavailability through the oral route.

© 2010 Elsevier B.V. All rights reserved.

1. Introduction

The anchoring of drug-loaded carriers at the mucosal surface by bioadhesive ligands to improve drug bioavailability has gained interest in the research of oral drug delivery systems. Ligand-mediated bioadhesive drug delivery systems can efficiently adhere to the mucus layer and surface of underlying cells, prolong residence time, and increase the drug concentration gradient between the particles and mucosal surface (Ponchel and Irache, 1998). Lectin is an excellent representative of such a specific ligand. It displays receptor-mediated bio-adhesion by recognizing and adhering to glycosylated structures, and may further convey signals to cells and trigger vesicular transport. Various lectins have been used in studies of oral drug delivery systems. These include tomato lectin (Lehr and Lee, 1993), peanut agglutinin (Cai and Zhang, 2005) and wheat germ agglutinin (WGA) (Irache et al., 1994), and the latter has been well investigated.

WGA binds specifically to *N*-acetyl-D-glucosamine and sialic acid. This adhesion may occur at cell surfaces throughout virtually the entire intestine (Pusztai et al., 1993). *In vitro* experiments using Caco-2 cells have revealed that the intracellular availability of WGA involves cyto-adhesion, cyto-invasion and partial lysosomal accumulation (Wirth et al., 2002). WGA in the microgram range does not show toxicity via the oral route, and is resistant to proteolytic degradation (Gabor et al., 1997). These features have ensured that WGA-grafted drugs (Gabor et al., 2002; Wirth et al., 1998) and WGA-decorated carrier systems (Weissenböck et al., 2004; Yin et al., 2007) have attracted much attention in recent years.

Colloidal lipid nanoparticles as carriers for drug delivery are characterized mainly by the narrow particle size and distribution of components (physiologically compatible lipids), biocompatibility, and administration routes (Gasco, 2007). It has been reported that lipid nanoparticles can enhance the oral absorption of drugs that are poorly soluble in water (Luo et al., 2006; Li et al., 2009) or proteins (Sarmento et al., 2007). Many factors contribute to the enhancement of oral bioavailability by lipid nanoparticles. These include: uptake of nanoparticles through the gastrointestinal tract (Li et al., 2009); lipid protection of the drug from degradation by chemicals or enzymes; improvement in intestinal absorption by surfactants in the drug formulation (Luo et al., 2006); and adhesion to the mucosal surface or entering intervallic spaces due to small particle size (Lim et al., 2004). The adhesion action by pure lipid nanoparticles is non-specific. Achieving effective attachment to the intestinal mucosal is difficult. Further improvement of the absorption and bioavailability of the drug by specific bio-adhesion is worth investigating. WGA as a functional ligand is conjugated with lipid nanoparticles to give rise to specific bio-adhesion between lipid nanoparticles and the surface of the cell membrane.

* Corresponding author. Tel.: +86 21 5132 2198; fax: +86 21 5132 2198.
E-mail address: npfeng@hotmail.com (N. Feng).

0378-5173/$ – see front matter © 2010 Elsevier B.V. All rights reserved.
doi:10.1016/j.ijpharm.2010.06.030

Another key issue is how to graft WGA with lipid nanoparticles: covalent coupling and physical adsorption are two strategies to achieve this goal (Ezpeleta et al., 1996). The former is preferentially more stable than non-covalent attachment. For covalent coupling, glutaraldehyde and carbodiimide coupling are the two most useful methods according to the functional groups on the nanoparticle surface. In general, directly grafting WGA with common lipid nanoparticles is difficult due to the limited number of functional groups on the surface of nanoparticles. Zhang et al. (2006) therefore prepared WGA-modified solid lipid nanoparticles by conjugating WGA with *N*-glutaryl-phosphatidylethanolamine, and the resulting conjugates were used as a surfactant in the preparation of solid lipid nanoparticles.

In the present study, we tried to prepare alternative WGA-grafted lipid nanoparticles by first introducing a sufficient number of functional groups to the surface of lipid nanoparticles, followed by a covalent coupling procedure for WGA conjugation. Poly(vinyl alcohol) (PVA) is an amphiphilic polymeric surfactant frequently used as an emulsifier for preparing microspheres. As a polymeric surfactant, its emulsification capabilities are relatively low, but it possesses a high viscosity and dispersion capability in colloidal dispersion systems. PVA has been used as an emulsifier to prepare solid lipid nanoparticles (SLNs) by a solvent diffusion method, and it was suggested that PVA molecules in the aqueous phase were absorbed around the droplets to facilitate nanoparticle formation (Hu et al., 2002). More recently, PVA was used as an emulsifier to stabilize solid lipid nanoparticles (Rosenblatt and Bunjes, 2009). Thus, it seems that PVA may be used as an emulsifier in lipid nanoparticles; it can then associate with the surface of nanoparticles, providing hydroxyl groups for WGA conjugation.

Bufalin is a hydrophobic active component extracted from the Toad venom with significant anti-tumor effects (Masuda et al., 1995; Han et al., 2007), analgesic effect (Zhang et al., 1998). Its poor water solubility contributes to low and variable oral absorption, which limits its clinical application. The aim of the present study was to prepare bufalin-loaded WGA-grafted lipid nanoparticles to study physicochemical properties and *in vitro* release. Cellular responses using WGA-grafted lipid nanoparticles (including the association between WGA-graft lipid nanoparticles and Caco-2 monolayers) were investigated to understand the characteristics of the binding and uptake and to elucidate the mechanism of action.

2. Materials and methods

2.1. Materials

Bufalin (purity >98%) was purchased from Jiangxi Herbfine Hi-Tech Company Limited (Nanchang, China). Glutaraldehyde was provided by Shanghai Chemical Reagent Company Limited (Shanghai, China). PVA (molecular weight, 31,000–50,000; hydrolysis, 87–89%), WGA, Tween 80, 6-coumarin and *N*-acetyl-D-glucosamine were purchased from Sigma–Aldrich (St. Louis, MO, USA). Glyceryl palmito-stearate (Precirol® ATO 5), glyceryl monolinoleate (Maisine 35-1®) and oleoyl macrogolglycerides (Labrafil® M1944 CS) were generously supplied by Gattefosse France (Gennevilliers, France). RPMI 1640 medium, fetal bovine serum (FBS), L-glutamine, gentamycine, phosphate-buffered saline (PBS, pH 7.4), and trypsin–ethylenediamine tetra-acetic acid (trypsin–EDTA) solution were from Gibco Life Technologies (Grand Island, NY, USA). Double-distilled water was obtained from Millipore Simplicity Systems (Millipore, Bedford, MA, USA).

2.2. Preparation of lipid nanoparticles

Lipid nanoparticles were prepared by a high-pressure homogenization method. In brief, the lipid phase (consisting of Precirol ATO 5, Maisine 35-1, Labrafil M1944 CS, and the drug (0.5%, w/w)) was heated at 70 °C until it was totally melted. The aqueous phase containing Tween 80 and PVA solution in double-distilled water was simultaneously prepared at the same temperature. A pre-emulsion was prepared by dispersing the hot aqueous phase into the lipid phase at 70 °C under high-speed stirring at 10,000 rpm for 10 min using an Ultra Turrax® T25 machine (IKA, Staufen, Germany). The hot pre-emulsion was then immediately homogenized at 800 bar for 9 cycles by a high-pressure homogenizer (NS1001L, GEA, Parma, Italy). Finally, the dispersion was gently stirred until cooled to room temperature. Free PVA was isolated by the ultrafiltration device Vivaspin 6.0 (Sartorius Stedim Biotech SA, Aubagne, France) under gentle centrifugation at $3000 \times g$ for 25 min. Hydrophobic fluorescent 6-coumarin-loaded lipid nanoparticles used for the cell association study were prepared using the same method except that 6-coumarin (0.04%, w/w) was encapsulated instead of the drug.

2.3. Surface modification of the particles

WGA was covalently bound to lipid nanoparticles by the glutaraldehyde method with an appropriate modification, as previously described (Montisci et al., 2001; Gupta et al., 2006). Briefly, the lipid nanoparticles were firstly centrifuged by Vivaspin 6.0 device. The un-entrapped drug was removed during this ultracentrifugation process. Then, glutaraldehyde and H_2SO_4 0.3 M (4:1, v/v) were added drop-wise to the lipid suspension. The mixture was gently shaken for 20 min at 30 °C. It was then transferred to a dialysis bag (molecular weight cut-off of 12,000) and firmly closed. Powdered polyethylene glycol-20,000 (PEG-20,000) was used to carefully cover the entire dialysis bag to remove aqueous solution containing non-reacted glutaraldehyde. After ~90% of the aqueous solution had been removed, an appropriate amount of water was added to the dialysis bag and the latter firmly closed. The glutaraldehyde-removal process was repeated twice in the same way. WGA in PBS was added to the dispersion and incubated overnight at room temperature. WGA-grafted lipid nanoparticles were separated from free lectin by passing the dispersion through a Sepharose CL-4B gel column. Aliquots of fresh preparations containing lactose as a cryoprotectant were rapidly frozen at less than −50 °C and freeze-dried for 48 h by a TF-FD-18 freeze dryer (Shanghai Tianfeng, Shanghai, China). Freeze-dried powders were collected for differential scanning calorimetry (DSC) analyses and X-ray powder diffraction (XRD) analyses.

2.4. Characterization of nanoparticles

The size and zeta potential of the lipid nanoparticles and WGA-grafted lipid nanoparticles were measured by a Nicomp™ 380 ZLS Zeta Potential/Particle Sizer (PSS Nicomp, Santa Barbara, CA, USA).

An ultrafiltration method was used to evaluate the encapsulation efficiency for lipid nanoparticles. Compared with the ultracentrifugation technique and gel permeation chromatography technique, the ultrafiltration method can provide efficient separation of colloidal carriers from the aqueous external phase without destroying the carriers thereof (Teeranachaideekul et al., 2007). Centrifugal filter tubes (molecular weight cut-off, 100 kDa; Nanosep®, Pall Life Sciences, Ann Arbor, MI, USA) were used to determine the encapsulation efficiency. The encapsulation efficiency was calculated according to the following equation (Arbós et al., 2002):

$$\text{encapsulation efficiency}\,(\%) = \frac{A_T - A_F}{A_T} \times 100$$

where A_T represents the total amount of bufalin used to prepare the formulations; and A_F represents the amount of free bufalin remaining in the aqueous phase after isolation.

The concentration of bufalin was determined by high-performance liquid chromatography (HPLC; Agilent 1100 series, Agilent, Santa Clara, CA, USA) on an ODS column (C_{18}, 250 mm × 4.6 mm, 5 μm; Dikma Technology, Shanghai, China). A mobile phase of methanol/water (70:30, v/v) was pumped at a flow rate of 1.0 mL/min. The detector was set at 300 nm.

The amount of bound WGA was quantified by colorimetric determination of the proteins in the nanoparticle dispersion by the bicinchoninic protein assay (BCA Protein Assay Kit, Thermo Scientific, Rockford, IL, USA). A non-conjugated nanoparticle dispersion was used as a control.

DSC analyses were carried out using a DSC calorimeter (Shimadzu DSC-60, Shimadzu, Japan). The sample was sealed in an aluminum DSC pan. The reference was an empty aluminum pan. The measurement was run at a heating rate of 10 °C/min.

XRD analyses were run in an X-ray diffractometer (D/max 2550VB3+/PC, Rigaku, Japan) using a CuKα radiation source. The voltage and current were 40 kV and 100 mA, respectively. The scan rate was 8 °C/min with 2θ scanning from 3° to 50°.

2.5. In vitro release

A dialysis bag diffusion method was applied to determine the release of bufalin from lipid nanoparticles. Two milliliters of preparations was transferred to a pre-treated dialysis bag with a molecular weight cut-off of 14 kDa. The bag was firmly clipped by dialysis clamps and immersed in a release medium composed of 50 mL of phosphate buffer (pH 7.4) containing 40% ethanol to achieve sink conditions. Vials were firmly closed and kept at 37 °C in a shaker water bath (100 strokes/min). At scheduled time intervals, 200 μL of the aqueous solution was withdrawn from the release medium and replaced with the same volume of fresh medium. Bufalin content in the release medium was determined by HPLC.

2.6. Cell culture

Caco-2 cells were kindly provided by Professor Hai Wei (Center of Chinese Medicine Therapy and Systems Biology, Shanghai University of TCM, Shanghai, China). Caco-2 cells were cultured in RPMI 1640 medium supplemented with 10% FBS, 4 mM L-glutamine, and 150 μg/mL gentamycine. Cells were incubated in a humidified atmosphere of 5% CO_2/95% air at 37 °C and sub-cultured to a sub-confluent state by trypsinization. Cells at passages 30–40 were used for subsequent experiments.

2.7. Association with Caco-2 monolayers

Caco-2 cell monolayers, representing an artificial gastrointestinal epithelium, were used to investigate the association of WGA-grafted lipid nanoparticles with cells. Experiments were carried out according to previously reported methods (Arbós et al., 2002; Dong and Feng, 2005). Caco-2 cells were seeded in a tissue culture (TC)-treated 96-well microplate (Greiner Bio-One, Solingen-Wald, Germany) at 1.7×10^4 cells per well. The culture medium was changed every other day. Cells after culture for 12–14 days were used to carry out the following experiment. In brief, the medium was removed. Cells were washed with PBS thrice. After removing PBS, 100 μL of the 80 μg/mL 6-coumarin-loaded formulation was added to 16 wells and incubated at 37 °C. At designated times, the supernatants of 8 wells were removed as samples for investigation (I_{sample}), whereas another 8 wells were kept intact as the positive control ($I_{positive}$). After removal of supernatants, cells were washed thrice with PBS (pH 7.4). Then, 50 μL of 0.5% Triton X-100/0.2 M NaOH was introduced into the wells to solubilize the cells. Fluorescence was determined by a microplate fluorescence reader (Synergy 2, BioTek, Winooski, VT, USA). The association efficiency of the cells was calculated as follows:

$$\text{Association efficiency}\,(\%) = \frac{I_{sample} - I_{negative}}{I_{positive} - I_{negative}} \times 100$$

where $I_{negative}$ indicates the background fluorescence intensity obtained from the plate and cells incubated with PBS.

Association of the preparations with monolayers was also studied at 4 °C to investigate the influence of temperature on association. To evaluate the specific binding of WGA-grafted lipid nanoparticles to Caco-2 monolayers, *N*-acetyl-D-glucosamine (an inhibitor of WGA binding to Caco-2 monolayers) was added to the incubation medium, and the experiment carried out as described above.

2.8. Confocal laser scanning microscopy (CLSM)

Caco-2 cells were cultured on glass-bottom dishes until they reached 50–70% confluence. Cells were incubated in WGA-free lipid nanoparticle dispersions (50 μL) or WGA-grafted lipid nanoparticle dispersions (50 μL) in fresh culture medium (1 mL) for 1, 3, and 24 h. The culture medium was removed and rinsed with PBS. Cells were fixed with ice-cold 4% paraformaldehyde in PBS (pH 7.4) for 25 min at room temperature, and rinsed with PBS. RNAs were digested by the addition of 400 μL RNase A solution (1 mg/mL) containing 0.1% Triton X-100 for 25 min at 37 °C. Subsequently, propidium iodide solution (PI; a nucleic acid-specific dye for nuclear DNA staining) was added to RNase A solution (final concentration of PI, 150 μg/mL) and cultured continuously for 2 min at 37 °C. Cells were washed with PBS and stored at 4 °C. Images were obtained under a confocal microscope (TCS SP2, Leica, Mannheim, Germany) using a fluorescein isothiocyanate (FITC) channel and tetramethyl rhodamine isothiocyanate (TRITC) channel for green fluorescence from 6-coumarin and red fluorescence from PI, respectively.

3. Results and discussion

3.1. Preparation of lipid nanoparticles and WGA-grafted lipid nanoparticles

Lipid nanoparticles were prepared by a high-pressure homogenization method. Based on a preliminary study, production parameters (homogenizer speed, number of cycles, homogenization pressure) and the basic formulation composition were determined. The optimized formulation composition obtained by uniform design was Precirol ATO 5, Maisine 35-1 and Labrafil® M1944 CS (5:1:1, w/w/w) of 5%, Tween 80 of 2.4%, and PVA of 0.25%.

WGA was covalently coupled to lipid nanoparticles according to the following steps as previously described (Montisci et al., 2001; Gupta et al., 2006): upon a strong adsorbed layer over lipid nanoparticles formed by PVA, a crosslinking reaction occurs via two adjacent hydroxyl groups with the aldehyde groups of the glutaraldehyde, followed by a coupling reaction between the free aldehyde groups and an amino group of WGA. The schematic of covalent linkage of WGA with lipid nanoparticles was shown as follows (Fig. 1):

First, PVA was used to provide hydroxyl groups as functional groups. As a polymeric surfactant, PVA was assumed to be covered to the surface of the lipid nanoparticles. Before the coupling reaction, the extent of PVA covering was studied by an ultrafiltration method. The amount of PVA was determined using a colorimetric assay with iodine and boric acid (Buttini et al., 2008) (Fig. 2).

The amount of PVA associated to lipid nanoparticles decreased significantly with increasing centrifugation, indicating that the extent of PVA coverage needs strength to remain attached to the

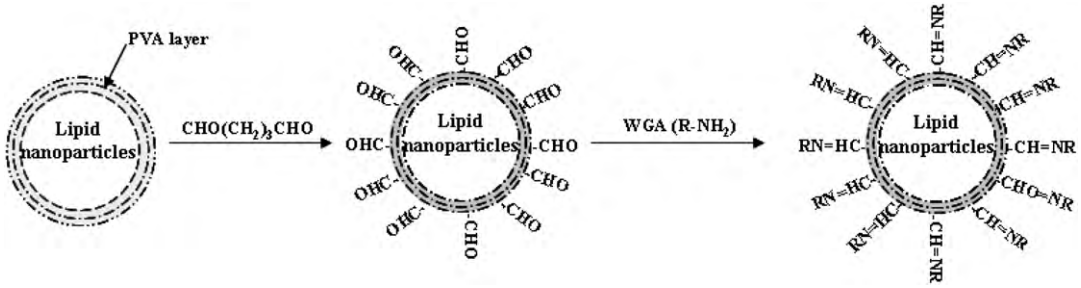

Fig. 1. The schematic of WGA conjugation with lipid nanoparticles.

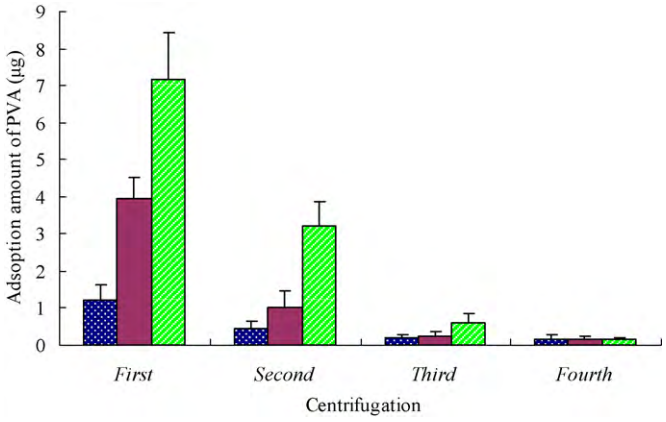

Fig. 2. Amount of PVA adsorbed onto the surface of lipid nanoparticles after centrifugation. The amount of PVA added before centrifugation was 6 μg ( ), 18 μg ( ), and 45 μg ( ) ($n = 3$).

lipid nanoparticles. Anchorage was reinforced by glutaraldehyde crosslinking to stabilize the PVA layer surrounding the core of the nanoparticles. This action is considered to strengthen the layer and may slow the drug release caused by crosslinking of PVA surrounding the core (Montisci et al., 2001). Thus, the release behavior of bufalin-loaded lipid nanoparticles before and after glutaraldehyde crosslinking was compared.

Bufalin release from lipid nanoparticles after the crosslinking reaction was significantly lower compared with the release without crosslinking (Fig. 3). There was no significant difference between the preparations lacking PVA with glutaraldehyde addition and the preparations containing PVA but without glutaraldehyde action. It was suggested that PVA crosslinking occurred at the particle surface, which may contribute to slow-down drug release from lipid nanoparticles.

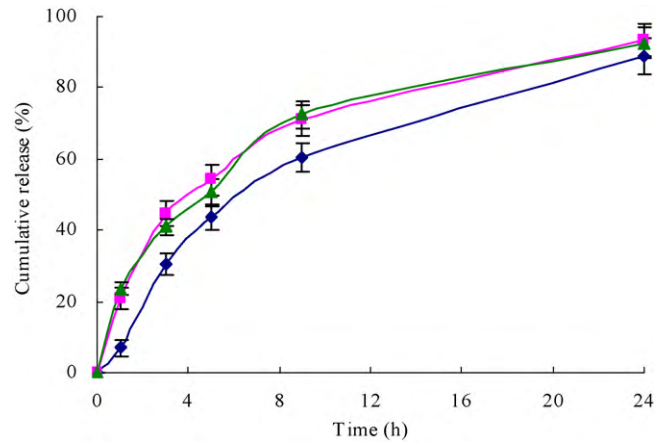

Fig. 3. *In vitro* release profile of bufalin from lipid nanoparticles with PVA in the aqueous phase without the glutaraldehyde crosslinking reaction ( ); with PVA in the aqueous phase with the glutaraldehyde crosslinking reaction ( ); without PVA in the aqueous phase with the glutaraldehyde crosslinking reaction ( ) ($n = 3$).

Glutaraldehyde was used not only as a crosslinking agent for PVA, but also as a coupling agent that provides free aldehyde groups for WGA conjugation. The non-reacted glutaraldehyde must be removed otherwise it may crosslink lectin molecules. It was reported previously that non-reacted glutaraldehyde was removed from polymer nanoparticles by high-speed centrifugation. In the present study, the condition of high-speed centrifugation was harsh, and would eventually result in particle aggregation or lipid separation against aqueous phases. To remove the non-reacted glutaraldehyde without destroying the lipid nanoparticles, an alternative method should be considered. One strategy is dialysis (Fischer and Scheer, 1992). To overcome the disadvantages of the traditional dialysis method (time-consuming, drug release), PEG-20,000 was covered on the surface of the dialysis bag instead of the dialysis bag being immersed in bulk aqueous solution. The influence of glutaraldehyde on WGA conjugation was also investigated. As shown in Table 1, when a constant amount of WGA was added initially and at a constant incubation time, the amount of coupled WGA increased with an increase in glutaraldehyde (Table 1), and the maximum binding efficiency of lectin was achieved when 2 mL of glutaraldehyde was used. However, the dispersion particle size in this case increased significantly. This indicated that the particle agglomeration may occur due to excessive crosslinking, which had a negative influence on the properties of lipid nanoparticles. Therefore, taking into account the efficiency of lectin binding and particle size, 1.5 mL of glutaraldehyde was selected and used in each milliliter of lipid nanoparticle dispersions after centrifugation.

The influence of the amount of lectin added to the activated dispersions on WGA binding to the lipid nanoparticles was also assessed (Table 1). An increase in WGA addition initially showed an increase in the amount of WGA bound to the surface. However, it significantly decreased the binding efficiency. Functional groups on the surface of nanoparticles were assumed to be constant and binding equilibrium may occur. However, binding equilibrium was not observed in the present study, and droplet size increased significantly. This result was in agreement with a report that proposed that aggregation occurred due to crosslinking of particles by a WGA molecule containing 24 amino groups (Weissenböck et al., 2004).

The amount of grafted WGA increased with incubation time without significantly altering the particle size (Table 1). According to these results, the experimental conditions to prepare WGA-grafted lipid nanoparticles were set as: 1.5 mL of glutaraldehyde, 400 μg of WGA added initially, and an incubation time of 18 h.

3.2. Characterization of WGA-grafted lipid nanoparticles

The main physicochemical characteristics of lipid nanoparticles and WGA-grafted lipid nanoparticles are listed in Table 2. The mean particle size of lipid nanoparticles before WGA coupling was

Table 1
Amount of WGA grafted onto lipid nanoparticles and binding efficiency.

Glutaraldehyde (mL)	WGA added initially, W_t (μg)	Incubation time (h)	Particle size (nm)	WGA grafted, W_g (μg)	Grafting efficiency (%)[a]
1.0	400	18	131.8 ± 6.9	52.2 ± 6.8	13.1
1.5	400	18	164.1 ± 5.2	115.6 ± 10.3	28.9
2.0	400	18	331.2 ± 8.1	136.8 ± 12.1	34.2
1.5	200	18	148.7 ± 3.8	82.7 ± 8.5	41.4
1.5	600	18	229.7 ± 11.6	138.6 ± 12.4	23.1
1.5	400	3	124.6 ± 7.7	34.1 ± 5.8	8.5

[a] Grafting efficiency (%) = $W_g/W_t \times 100$.

Table 2
Particle size, zeta potential and encapsulation efficiency of formulations.

Formulation	Particle size (nm)	Zeta potential (mV)	Encapsulation efficiency (%)
Lipid nanoparticles	106.0 ± 4.6	−19.2 ± 0.7	75.8 ± 0.9
WGA-grafted lipid nanoparticles	164.1 ± 5.2	−10.6 ± 1.2	68.2 ± 3.2

106 nm. The WGA-grafted lipid nanoparticles were larger, indicating that the conjugation of WGA increased particle size. The increase in particle size is acceptable because a mean particle size of 164 nm is in the nanometer range, so WGA-grafted lipid nanoparticles can be used as lipid-based colloidal drug carriers.

The zeta potential is also an important surface characteristic of lipid nanoparticles, and which reflects the particle charge and/or electrostatic repulsion. The zeta potential was measured to determine if surface characteristics are influenced by the nature of the coating of lipid nanoparticles. Before WGA conjugation, the zeta potential of lipid nanoparticles was −19.2 mV (Table 2), indicating that the surface of lipid nanoparticles was negatively charged. A decreased zeta potential was found after WGA binding, indicating that changes in the particle charge of lipid nanoparticles was due to WGA conjugation. WGA had a positive charge at neutral pH (*p*I 7.0), which may contribute to the decrease in the zeta potential for negatively charged lipid nanoparticles after WGA conjugation.

The encapsulation efficiency was calculated to be 75.8% before WGA conjugation. Lipid nanoparticles, particularly nanostructured lipid carriers (NLCs) are known to be a favorable system for drug incorporation. It was reported that solid lipid nanoparticles or NLCs containing hydrophobic drugs with such as quercetin (Li et al., 2009), vinpocetine (Luo et al., 2006), and coenzyme Q_{10} (Teeranachaideekul et al., 2007) were well incorporated into lipid carriers and achieved an encapsulation efficiency of >90%. The hydrophobic drugs mentioned above possess high partition coefficients and have good compatibility with lipid matrices, resulting in high encapsulation efficiency. In our preliminary study, it was found that bufalin displayed moderate lipophilicity (log *P* (octanol/water) of 2.9). If drugs with low or moderate lipophilicity are dispersed in a system composed of oils and surfactants at high temperature during preparation, drug molecules tend to partition into the aqueous phase, resulting in relatively lower encapsulation efficiency. Furthermore, the encapsulation efficiency of bufalin in lipid nanoparticles was found to be significantly higher than that in polymeric nanoparticles (data not shown), indicating that lipid nanoparticles are a suitable carrier for this study. In addition, a slight decrease in encapsulation efficiency was found in WGA-grafted lipid nanoparticles compared with that in pure lipid nanoparticles due to the preparation process.

DSC can be used to determine thermodynamic variations related to morphological changes. It has been used successfully to demonstrate the melting and crystallization behavior of lipid matrices, the constitution of lipid nanoparticles (i.e., organization and distribution of lipid ingredients) and drug collocation (Castelli et al., 2005; Zhang et al., 2008; Helgason et al., 2009). In the present study, DSC was carried out to investigate the melting and crystallization behavior of lipid nanoparticles and drug collocation. Bulk Precirol ATO 5 showed an endothermic peak for melting at 56.3 °C (Fig. 4(a)) whereas, in the case of WGA-grafted lipid nanoparticles, the shape of the peak became broader and lower (Fig. 4(c) and (d)). Disappearance of a sharp peak suggested that a less ordered crystal structure existed in lipid nanoparticles compared with the perfectly crystalline substance. The DSC curve of bufalin exhibited an endothermic peak at 231.1 °C (Fig. 4(b)). The same melting peak did not appear when it was formulated into lipid nanoparticles (Fig. 4(d)). This indicates that bufalin entrapped in the lipid nanoparticles was in an amorphous from, which may have been caused by crystallization inhibition from the lipid components, as previously described (Venkateswarlu and Manjunath, 2004).

Analyses of XRD patterns were carried out to further investigate the microstructure of WGA-grafted lipid nanoparticles. The X-ray patterns of Precirol ATO 5, PVA, and blank WGA-grafted lipid nanoparticles are shown in Fig. 5. From Fig. 5(a), the bulk Precirol ATO 5 showed two peaks at positions 5.36° (2θ) and 19.44° (2θ), respectively, whereas in Fig. 5(c) the peak at 5.36° disappeared and the peak located at 19.44° shifted to a lower position. The peak intensity decreased significantly in Fig. 5(c) compared with that in Fig. 5(a). From these results, it was confirmed that Precirol ATO 5 was in a less ordered structure in lipid nanoparticles. The X-ray

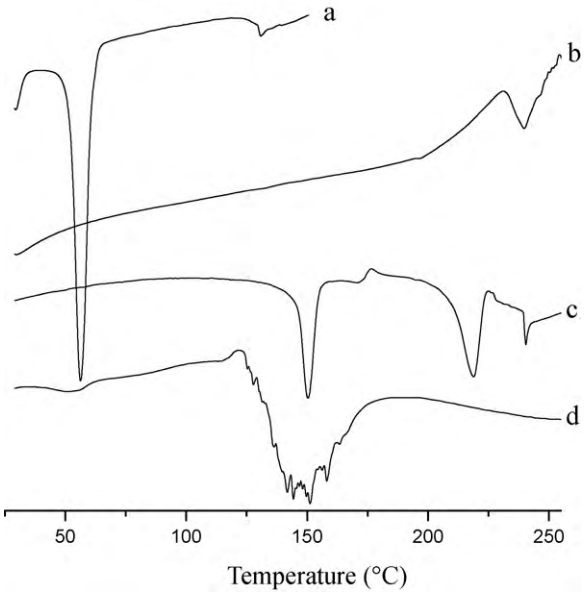

Fig. 4. DSC curves of (a) Precirol ATO 5; (b) bufalin; (c) lactose; and (d) bufalin-loaded WGA-grafted lipid nanoparticles.

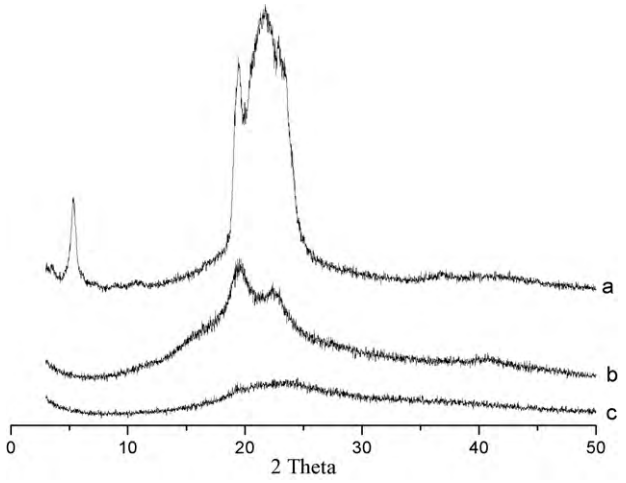

Fig. 5. X-ray diffraction patterns of (a) Precirol ATO 5; (b) PVA; and (c) blank WGA-grafted lipid nanoparticles.

pattern of PVA showed a typical amorphous state with two blunt, broad peaks with low slopes (Fig. 5(b)). From Fig. 5(c), it seems that PVA remained in an amorphous state in lipid nanoparticles.

3.3. In vitro release

WGA is soluble in the aqueous external phase, so WGA should not influence drug release from lipid nanoparticles (Mo and Lim, 2005). In the present study, activated lipid nanoparticles were used for drug release studies (Fig. 3). In general, drug properties and the nature of the lipid carriers contribute to the release of drug from a lipid-based drug delivery system. It was reported that the drug location in the lipid nanocarrier is related to the polar surface area of the drug molecule, i.e., the sum of the surfaces from polar atoms in a molecule (Pegi et al., 2003; Teskač and Kristl, 2010). Bufalin is predominantly hydrophobic, but has two hydroxyl groups. Bufalin could therefore be located at the interface of the dispersions. From this viewpoint, it was deduced that not all bufalin molecules are incorporated into the core of lipid nanoparticles, and that some of molecules may be entrapped in the shell (possibly causing the relatively fast release in the first 3 h). According to our previous report (Liu et al., 2010a), the drug release from a bufalin self-microemulsifying drug delivery system (SMEDDS) was very rapid, and 90% of the drug was released in the first 2 h. Bufalin release from lipid nanoparticles is much slower than that from SMEDDS, indicating that the nature of the lipid carrier plays an important part in drug release. Lipid nanoparticles are more favorable for controlling drug release from carriers. To achieve a sink condition, the dissolution media containing 40% (v/v) ethanol was used. It should be noted that the choice of dissolution media still needs investigation due to its poor ability in simulating *in vivo* conditions, and it would be very interesting to seek desirable dissolution media which fulfill complete release and simulate *in vivo* condition as well.

3.4. Binding and uptake

Caco-2 cells are derived from human colon carcinomas. They are widely used in pharmaceutical technology to mimic the intestinal epithelium *in vitro*. In the present study, a Caco-2 cell culture model was used to evaluate the association between WGA-grafted lipid preparations and cells. Before the association study, a suitable fluorescent material should be selected. In general, the fluorescent material is coupled to nanoparticles by covalent conjugation with one of the components in the formulation. FITC conjugate is frequently used in uptake or fluorescence microscopy studies on

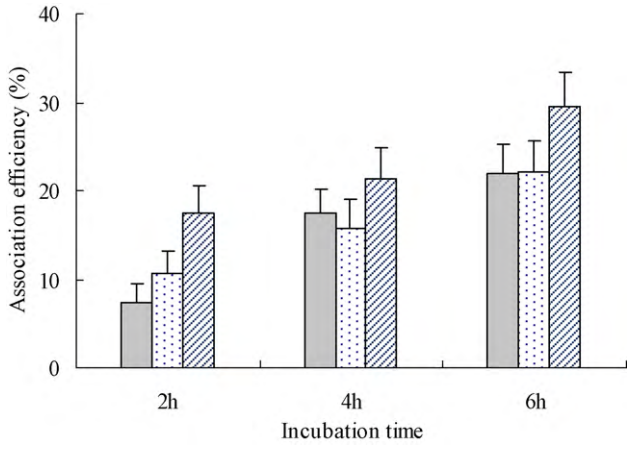

Fig. 6. Association efficiency between Caco-2 monolayers and WGA-free lipid nanoparticles ( ), BSA-grafted lipid nanoparticles ( ) and WGA-grafted lipid nanoparticles ( ) at 37 °C.

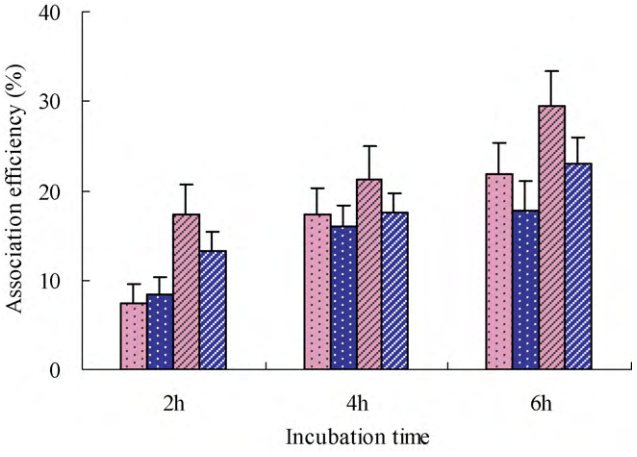

Fig. 7. Association efficiency between Caco-2 monolayers and WGA-free lipid nanoparticles at 37 °C ( ), WGA-free lipid nanoparticles at 4 °C ( ), WGA-grafted lipid nanoparticles at 37 °C ( ), and WGA-grafted lipid nanoparticles at 4 °C ( ).

nanoparticles. Another simple way is to incorporate a hydrophobic fluorescent material (e.g., nile red, bodipy, rhodamine, 6-coumarin) directly into lipid nanoparticles. In the present study, 6-coumarin was loaded in lipid nanoparticles and release of the former from

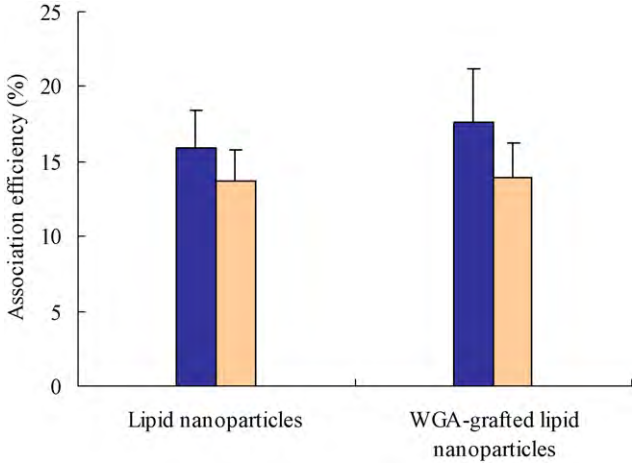

Fig. 8. Association efficiency between Caco-2 monolayers and WGA-free lipid nanoparticles and WGA-grafted lipid nanoparticles with *N*-acetyl-D-glucosamine ( ) or without *N*-acetyl-D-glucosamine ( ) at 4 °C.

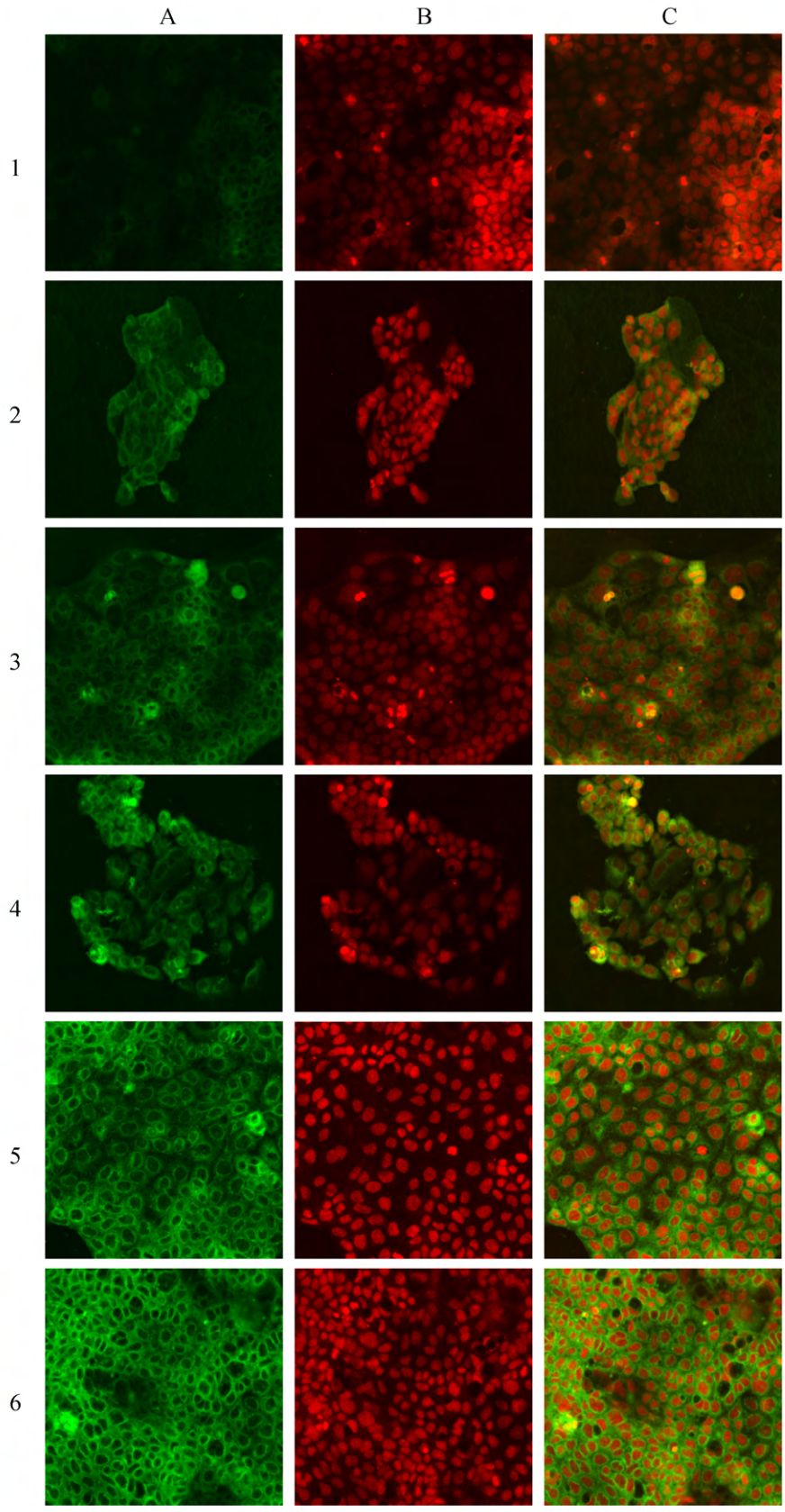

Fig. 9. Confocal laser scanning microscopy images of Caco-2 cells. Rows 1, 3, 5 show the images of Caco-2 cells incubated with WGA-free lipid nanoparticles at 1, 3, and 24 h, respectively; rows 2, 4, and 6 show the images of Caco-2 cells incubated with WGA-grafted lipid nanoparticles at 1, 3, and 24 h, respectively. Columns A, B, and C show the images from the FITC channel, TRITC channel, and the merged images, respectively (⟵⟶ 75 μm).

nanoparticles determined. It was found that <1% of 6-coumarin was released in the first 24 h. That is, the fluorescence intensity detected during the association study experiment was originally from the 6-coumarin loaded in nanoparticles rather than from the free fluorescence in the supernatant. It has been reported that neat 6-coumarin cannot be directly internalized by cells (Dong and Feng, 2005). Thus, 6-coumarin was selected as a fluorescent material in the present study.

To assess the association between WGA-grafted lipid nanoparticles and Caco-2 cell monolayers, WGA-grafted lipid nanoparticles and formulations as control preparations, including WGA-free nanoparticles and bovine serum albumin (BSA; a non-specific protein)-grafted lipid nanoparticles were incubated with cell monolayers at 37 °C. For all three preparations, the association efficiency increased with incubation time (Fig. 6). There was no significant difference between WGA-free lipid nanoparticles and BSA-grafted lipid nanoparticles. The association of WGA-grafted lipid nanoparticles was approximately 1.5-fold higher than that of WGA-free nanoparticles or BSA-grafted nanoparticles. This indicated that WGA facilitated the association between lipid nanoparticles and cells.

Previous reports have suggested that WGA can adhere to the glycocalyx of Caco-2 cells and be further internalized by these cells. To examine if the WGA-grafted lipid nanoparticles in the present study could be internalized by cells, the influence of temperature on the association study was investigated from the viewpoint of understanding the mechanism of binding and uptake. Metabolic activity and the fluidity of the cell membrane at 4 and 37 °C are different. At 4 °C, the low metabolic activity and poor membrane fluidity result in restriction of active transport. Therefore, the association between cells and nanoparticles mainly refers to binding. At 37 °C, active transport (i.e., uptake) may occur due to active metabolism and increased membrane fluidity (Wirth et al., 2002). The efficiency of association between cells and nanoparticles at 37 °C was increased compared with that at 4 °C for both preparations (Fig. 7). For WGA-grafted lipid nanoparticles, the increased association was much higher, indicating that more WGA-grafted lipid nanoparticles were delivered into cells by active transport, and that the transport was energy-dependent.

To further examine the specific association of WGA-grafted lipid nanoparticles with Caco-2 monolayers, the WGA inhibitory sugar *N*-acetyl-D-glucosamine was used on cells before the association study; the association study of WGA-grafted lipid nanoparticles was carried out with WGA-free lipid nanoparticles as a control at 4 °C. The addition of *N*-acetyl-D-glucosamine significantly reduced the association efficiency (Fig. 8). It also suggested that WGA facilitated the association of lipid nanoparticles with cells. The association efficiency of WGA-free lipid nanoparticles under the action of *N*-acetyl-D-glucosamine also slightly decreased compared with that without addition of *N*-acetyl-D-glucosamine. This phenomenon was also observed in another report; the reasons proposed for this effect were changes in surface area or high osmotic gradients caused by *N*-acetyl-D-glucosamine to the cells (Arbós et al., 2002).

3.5. CLSM

Fluorescent microscopy studies were carried out to better understand and visualize the cellular uptake of WGA-grafted lipid nanoparticles. Caco-2 cells were incubated with WGA-grafted lipid nanoparticles and WGA-free lipid nanoparticles at 37 °C for different time intervals followed by observation by CLSM (Fig. 9). The green image in column 1 is the fluorescence from 6-coumarin-loaded nanoparticles, and the red image in column 2 is caused by PI staining the nuclei. Column 3 is the merged image of columns 1 and 2. Rows 1, 3, and 5 list images of cells incubated with WGA-free lipid nanoparticles at 1, 3, and 24 h, respectively. Rows 2, 4, 6 list the images of cells incubated with WGA-grafted lipid nanoparticles at 1, 3, and 24 h, respectively. The fluorescence intensity was weak and some cells were not detectable for 6-coumarin green fluorescence in rows 1 and 2, indicating that only a few nanoparticles had been internalized by the cell in 1 h. Compared with the images of cellular uptake in 1 h, a more intense green fluorescence around the nucleus was observed at 3-h incubation (rows 3 and 4). The fluorescence intensity of cells incubated with WGA-grafted lipid nanoparticles was obviously stronger than that with WGA-free lipid nanoparticles. These results suggested that cellular uptake of lipid nanoparticles were time-dependent, and that WGA facilitated uptake of lipid nanoparticles by cells. This was further confirmed by confocal images of cells incubated with WGA-grafted lipid nanoparticles or WGA-free nanoparticles for 24 h. The process and mechanism of nanoparticle uptake by cells via fluid-phase endocytosis, receptor-mediated endocytosis, and phagocytosis have been reported (Weissleder et al., 1997; Schoepf et al., 1998; Liu et al., 2010b). Targeting cells and enhancing the cellular uptake of nanoparticles through receptor-mediated endocytosis is a promising strategy. WGA was used as a ligand in the present study. The interaction of WGA with Caco-2 cells has been investigated (Wirth et al., 2002). It was proposed that, upon contact with the cell membrane, WGA is specifically bound to the glycocalyx, and uptake occurs after cyto-adhesion, then cyto-invasion enables the WGA to accumulate in acid lysosomal compartments. We observed cellular uptake of WGA-grafted lipid nanoparticles. The intracellular distribution and fate of the internalized nanoparticles needs further investigation.

4. Conclusion

A method for the preparation of WGA-grafted lipid nanoparticles was established. The physicochemical characteristics of nanoparticles were assessed. Particles had a size of ~164 nm and a zeta potential of −10.6 mV. DSC and XRD analyses revealed the structure of lipid nanoparticles, with the existence of a less well-ordered crystalline state and a mainly amorphous arrangement. The *in vitro* release profile showed the typical release behavior of lipid nanoparticles. The association study between Caco-2 monolayers and lipid nanoparticles showed that WGA enhanced the binding and uptake of lipid nanoparticles with cells. This suggested that an energy-dependent mechanism and sugar-specific interaction may contribute to the enhanced association of WGA-grafted lipid nanoparticles with cells.

Acknowledgements

This work was supported by grants (szy06022 and J50302) from Shanghai Education Committee, Program (10XD1403900) of Shanghai Subject Chief Scientist, and Program (NCET-08-0898) for New Century Excellent Talents of the State Education Ministry, PR China. The authors gratefully acknowledge Prof. Yong Gan and Dr. Xin-xin Zhang of Shanghai Institute of Material Medica and Dr. Yue Wang of China Pharmaceutical University for their generous support and suggestions.

References

Arbós, P., Wirth, M., Arangoa, M.A., Gabor, F., Irache, J.M., 2002. Gantrez® AN as a new polymer for the preparation of ligand-nanoparticle conjugates. J. Control. Release 83, 321–330.

Buttini, F., Soltani, A., Colombo, P., Marriott, C., Jones, S.A., 2008. Multilayer PVA adsorption onto hydrophobic drug substrates to engineer drug-rich microparticles. Eur. J. Pharm. Sci. 33, 20–28.

Cai, Q., Zhang, Z.R., 2005. Lectin-mediated cytotoxicity and specificity of 5-fluorouracil conjugated with peanut agglutinin (5-Fu-PNA) *in vitro*. J. Drug Target. 13, 251–257.

Castelli, F., Puglia, C., Sarpietro, M.G., Rizza, L., Bonina, F., 2005. Characterization of indomethacin-loaded lipid nanoparticles by differential scanning calorimetry. Int. J. Pharm. 304, 231–238.

Dong, Y., Feng, S.S., 2005. Poly(D,L-lactide-co-glycolide)/montmorillonite nanoparticles for oral delivery of anticancer drugs. Biomaterials 26, 6068–6076.

Ezpeleta, I., Irache, J.M., Stainmesse, S., Chabenat, C., Gueguen, J., Orecchioni, A.M., 1996. Preparation of lectin–vicilin nanoparticle conjugates using the carbodiimide coupling technique. Int. J. Pharm. 142, 227–233.

Fischer, R., Scheer, H., 1992. Dissociating effect of chromophore modifications on C-Phycocyanin. J. Photochem. Photobiol. 15, 91–103.

Gabor, F., Wirth, M., Jurkovich, B., Haberl, I., Theyer, G., Walcher, G., Haberl, I., Theyer, G., Walcher, G., Hamilton, G., 1997. Lectin-mediated bioadhesion: proteolytic stability and binding-characteristics of wheat germ agglutinin and Solanum tuberosum lectin on Caco-2, HT-29 and human colonocytes. J. Control. Release 49, 27–37.

Gabor, F., Schwarzbauer, A., Wirth, M., 2002. Lectin-mediated drug delivery: binding and uptake of BSA–WGA conjugates using the Caco-2 model. Int. J. Pharm. 237, 227–239.

Gasco, M.R., 2007. Lipid nanoparticles: perspectives and challenges. Adv. Drug Deliv. Rev. 59, 377–378.

Gupta, P.N., Mahor, S., Rawat, A., Khatri, K., Goyal, A., Vyas, S.P., 2006. Lectin anchored stabilized biodegradable nanoparticles for oral immunization. 1. Development and *in vitro* evaluation. Int. J. Pharm. 318, 163–173.

Han, K.Q., Huang, G., Gu, W., Su, Y.H., Huang, X.Q., Ling, C.Q., 2007. Anti-tumor activities and apoptosis-regulated mechanisms of bufalin on the orthotopic transplantation tumor model of human hepatocellular carcinoma in nude mice. World. J. Gastroenterol. 54, 3374–3379.

Helgason, T., Awad, T.S., Kristbergsson, K., McClements, D.J., Weiss, J., 2009. Effect of surfactant surface coverage on formation of solid lipid nanoparticles (SLN). J. Colloid Interface Sci. 334, 75–81.

Hu, F.Q., Yuan, H., Zhang, H.H., Fang, M., 2002. Preparation of solid lipid nanoparticles with clobetasol propionate by a novel solvent diffusion method in aqueous system and physicochemical characterization. Int. J. Pharm. 339, 121–128.

Irache, J.M., Durrer, C., Duchêne, D., Ponchel, G., 1994. *In vitro* study of lectin–latex conjugates for specific bioadhesion. J. Control. Release 31, 181–188.

Lehr, C.M., Lee, V.H., 1993. Binding and transport of some bioadhesive plant lectins across Caco-2 cell monolayers. Pharm. Res. 10, 1796–1799.

Li, H., Zhao, X., Ma, Y., Zhai, G., Li, L., Lou, H., 2009. Enhancement of gastrointestinal absorption of quercetin by solid lipid nanoparticles. J. Control. Release 133, 238–244.

Lim, S.J., Lee, M.K., Kim, C.K., 2004. Altered chemical and biological activities of all-trans retinoic acid incorporated in solid lipid nanoparticle powders. J. Control. Release 100, 53–61.

Liu, Y., Chen, Z.Q., Zhang, X., Feng, N.P., Zhao, J.H., Wu, S., Tan, R., 2010a. An improved formulation screening and optimization method applied to the development of a self-microemulsifying drug delivery system. Chem. Pharm. Bull. 58, 16–22.

Liu, Y., Li, K., Pan, J., Liu, B., Feng, S.S., 2010b. Folic acid conjugated nanoparticles of mixed lipid monolayer shell and biodegradable polymer core for targeted delivery of Docetaxel. Biomaterials 31, 330–338.

Luo, Y., Chen, D., Ren, L., Zhao, X., Qin, J., 2006. Solid lipid nanoparticles for enhancing vinpocetine's oral bioavailability. J. Control. Release 114, 53–59.

Masuda, Y., Kawazoe, N., Nakajo, S., Yoshida, T., Nakaya, K., 1995. Bufalin induces apoptosis and influences the expression of apoptosis-related genes in human leukemia cells. Leuk. Res. 19, 549–556.

Mo, Y., Lim, L.Y., 2005. Preparation and *in vitro* anticancer activity of wheat germ agglutinin (WGA)-conjugated PLGA nanoparticles loaded with paclitaxel and isopropyl myristate. J. Control. Release 107, 30–42.

Montisci, M.J., Giovannuci, G., Duchêne, D., Ponchel, G., 2001. Covalent coupling of asparagus pea and tomato lectins to poly(lactide) microspheres. Int. J. Pharm. 215, 153–161.

Pegi, A., Julijana, K., Slavko, P., Janez, S., Marjeta, S., 2003. The effect of lipophilicity of spin-labeled compounds on their distribution in solid lipid nanoparticle dispersions studied by electron paramagnetic resonance. J. Pharm. Sci. 92, 58–66.

Ponchel, G., Irache, J., 1998. Specific and non-specific bioadhesive particulate systems for oral delivery to the gastrointestinal tract. Adv. Drug Deliv. Rev. 34, 191–219.

Pusztai, A., Ewen, S.W., Grant, G., Brown, D.S., Stewart, J.C., Peumans, W.J., Van Damme, E.J.M., Bardocz, S., 1993. Antinutritive effects of wheat-germ agglutinin and other N-acetylglucosamine-specific lectins. Br. J. Nutr. 70, 313–321.

Rosenblatt, K.M., Bunjes, H., 2009. Poly(vinyl alcohol) as emulsifier stabilizes solid triglyceride drug carrier nanoparticles in the α-modification. Mol. Pharm. 6, 105–120.

Sarmento, B., Martins, S., Ferreira, D., Souto, E.B., 2007. Oral insulin delivery by means of solid lipid nanoparticles. Int. J. Nanomed. 2, 743–749.

Schoepf, U., Marecos, E.M., Melder, R.J., Jain, R.K., Weissleder, R., 1998. Intracellular magnetic labeling of lymphocytes for *in vivo* trafficking studies. Biotechniques 24, pp. 642–646, 648–651.

Teeranachaideekul, V., Souto, E.B., Junyaprasert, V.B., Müller, R.H., 2007. Cetyl palmitate-based NLC for topical delivery of Coenzyme Q_{10}-development, physicochemical characterization and *in vitro* release studies. Eur. J. Pharm. Biopharm. 67, 141–148.

Teskač, K., Kristl, J., 2010. The evidence for solid lipid nanoparticles mediated cell uptake of resveratrol. Int. J. Pharm. 390, 61–69.

Venkateswarlu, V., Manjunath, K., 2004. Preparation, characterization and *in vitro* release kinetics of clozapine solid lipid nanoparticles. J. Control. Release 95, 627–638.

Weissenböck, A., Wirth, M., Gabor, F., 2004. WGA-grafted PLGA-nanospheres: preparation and association with Caco-2 single cells. J. Control. Release 99, 383–392.

Weissleder, R., Cheng, H.C., Bogdanova, A., Bogdanov A.Jr., 1997. Magnetically labeled cells can be detected by MR imaging. J. Magn. Reson. Imaging 7, 258–263.

Wirth, M., Fuchs, A., Wolf, M., Ertl, B., Gabor, F., 1998. Lectin-mediated drug targeting: preparation, binding characteristics, and antiproliferative activity of wheat germ agglutinin conjugated doxorubicin on Caco-2 cells. Pharm. Res. 15, 1031–1037.

Wirth, M., Kneuer, C., Lehr, C.M., Gabor, F., 2002. Lectin-mediated drug delivery: discrimination between cytoadhesion and cytoinvasion and evidence for lysosomal accumulation of wheat germ agglutinin in the Caco-2 model. J. Drug Target. 10, 439–448.

Yin, Y., Chen, D., Qiao, M., Wei, X., Hu, H., 2007. Lectin-conjugated PLGA nanoparticles loaded with thymopentin: *ex vivo* bioadhesion and *in vivo* biodistribution. J. Control. Release 123, 27–38.

Zhang, W., Liu, Y.L., Xu, C.Y., Gao, W., Bao, W.F., 1998. Research on the active analgesic component of venenum bufonis. Shenyang Yao Ke Da Xue Xue Bao 15, 268–271.

Zhang, N., Ping, Q., Huang, G., Xu, W., Cheng, Y., Han, X., 2006. Lectin-modified solid lipid nanoparticles as carriers for oral administration of insulin. Int. J. Pharm. 327, 153–159.

Zhang, X.X., Pan, W.S., Gan, L., Zhu, C.L., Gan, Y., Nie, S.F., 2008. Preparation of a dispersible PEGylate nanostructured lipid carriers (NLC) loaded with 10-hydroxycamptothecin by spray-drying. Chem. Pharm. Bull. 56, 1645–1650.